



THE UNIVERSITY *of* EDINBURGH

Edinburgh Research Explorer

Complementary Ionization Techniques for the Analysis of Scotch Whisky by High Resolution Mass Spectrometry

Citation for published version:

Kew, W, Mackay, CL, Goodall, I, Clarke, DJ & Uhrín, D 2018, 'Complementary Ionization Techniques for the Analysis of Scotch Whisky by High Resolution Mass Spectrometry', *Analytical Chemistry*.
<https://doi.org/10.1021/acs.analchem.8b01446>

Digital Object Identifier (DOI):

[10.1021/acs.analchem.8b01446](https://doi.org/10.1021/acs.analchem.8b01446)

Link:

[Link to publication record in Edinburgh Research Explorer](#)

Document Version:

Publisher's PDF, also known as Version of record

Published In:

Analytical Chemistry

General rights


Copyright for the publications made accessible via the Edinburgh Research Explorer is retained by the author(s) and / or other copyright owners and it is a condition of accessing these publications that users recognise and abide by the legal requirements associated with these rights.

Take down policy

The University of Edinburgh has made every reasonable effort to ensure that Edinburgh Research Explorer content complies with UK legislation. If you believe that the public display of this file breaches copyright please contact openaccess@ed.ac.uk providing details, and we will remove access to the work immediately and investigate your claim.



Complementary Ionization Techniques for the Analysis of Scotch Whisky by High Resolution Mass Spectrometry

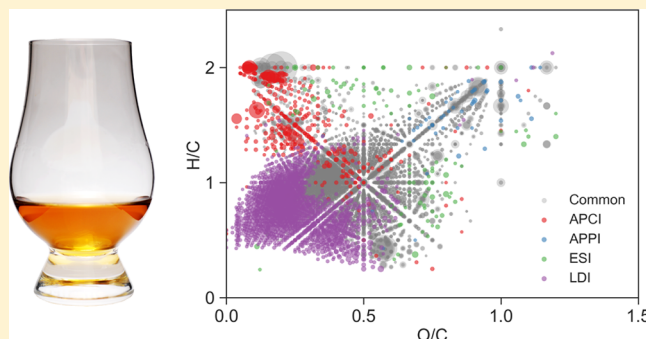
Will Kew,[†] C. Logan Mackay,[†] Ian Goodall,[‡] David J. Clarke,^{*,†} and Dušan Uhrín^{*,†} 

[†]EaStCHEM School of Chemistry, University of Edinburgh, Joseph Black Building, Edinburgh, United Kingdom, EH9 3FJ

[‡]The Scotch Whisky Research Institute, The Robertson Trust Building, Research Avenue North, Riccarton, Edinburgh, United Kingdom, EH14 4AP

Supporting Information

ABSTRACT: Fourier transform mass spectrometry (FTMS) is widely used to characterize the chemical complexity of mixtures, such as natural organic matter (NOM), petroleum, and agri-food products (including Scotch whisky). Although electrospray ionization (ESI) is by far the most widely used ionization source in these studies, other ionization techniques are available and may offer complementary information. In a recent study, we found matrix free laser desorption/ionization (LDI) to be effective for the analysis of Suwannee river fulvic acid (SRFA), and to provide complementary chemical insights. In this study, LDI along with atmospheric pressure photoionization (APPI) and atmospheric pressure chemical ionization (APCI) were compared to ESI for the analysis of Scotch whisky. High mass accuracy (54 ppb, mean) allowed for the assignment of 86% of peaks, with 3993 unique molecular formulas identified from four representative samples analyzed. All four ionization techniques, performed in negative mode, identified thousands of formulas. Many were unique to each ionization source, while 699 formulas were common to all techniques. Ions were identified in both deprotonated and radical anion forms. Our study highlights the importance of a multi-ionization source approach; we recommend that analysis of complex mixtures, especially novel ones, should not be limited solely to ESI.



Scotch whisky is a complex mixture containing low concentrations of thousands of small molecules. In a previous paper,¹ we demonstrated how negative electrospray ionization (ESI) Fourier transform ion cyclotron resonance mass spectrometry (FTICR-MS) could be used to identify the molecular formula of thousands of compounds in dozens of samples of Scotch whisky. Chemometric analysis of the mass spectra showed separation between blended whiskies and malt whiskies, as well as differentiation between maturation wood types. The choice of negative ESI was deliberate, reflecting what is the most commonly used ionization technique in complex mixture analysis. Positive and negative mode ESI FTICR-MS was previously used to investigate Scotch whisky brand differences and to address authentication concerns.² In that work, positive mode ions were largely assigned to singly charged CHO formulas with sodium adducts ($[M + Na]^+$). In accord with our experience, negative mode ESI produced predominantly singly charged and deprotonated ions ($[M - H]^-$). Very recently, negative ESI has again been used to characterize a large set of whisky and rum samples.³ ESI in both polarities had also been coupled with time-of-flight (TOF) mass spectrometry (MS), showing the ability to fingerprint Scotch whisky.⁴ ESI has also been used for the analysis of other food and drink products, including beer,⁵

wine, and champagne,^{6–8} and pet food.⁹ The more general use of high-resolution mass spectrometry in “foodomics” has been reviewed,¹⁰ and this approach has been proposed to investigate the mycobolome.¹¹

The ubiquity of ESI in complex mixture analysis is well-known; however, other ionization methods exist, potentially affording complementary information. These include solution-state techniques such as atmospheric pressure photoionization (APPI), atmospheric pressure chemical ionization (APCI), and solid-state matrix assisted laser desorption ionization (MALDI).

APPI and APCI have been applied for the analysis of natural organic matter (NOM),¹² lignin,^{13,14} and petroleum.^{15,16} APPI in the positive mode has been used to characterize porphyrins in petroleum,¹⁷ generated data sets of crude oils for statistical analysis,¹⁵ and has been used to acquire the most complex assigned spectrum to date, with over 126000 out of 170000 peaks assigned in a single sample of volcanic asphalt.¹⁸ Here, positive mode APPI was used as the asphalt sample was known to contain many less polar, nitrogen-containing species. The

Received: March 30, 2018

Accepted: September 6, 2018

Published: September 6, 2018

same ionization technique has also been used at 21 T in another study of asphalts.¹⁹ Negative ion APPI appears to be far less utilized in complex mixture analysis. APCI has also been utilized in positive mode for petroleum analysis¹⁶ and for the study of food (avocados) in combination with TOF mass spectrometry.^{20,21}

MALDI has been applied to complex mixture analysis of NOM.²² In a recent publication, we demonstrated that for Suwanee river fulvic acid (SRFA), a NOM sample, matrix-free laser desorption ionization (LDI) not only worked, but outperformed traditional MALDI in terms of spectral quality, sensitivity, and lack of contaminants.²³ In that study, LDI performed as a soft ionization technique, producing no observable fragmentation. That a MALDI matrix was unnecessary was rationalized by the abundance of small molecules with aromatic moieties in SRFA, as demonstrated by Witt et al.²⁴ and others.²⁵ We proposed that these molecules were sufficient to promote ionization. Many of the aromatic molecules are lignin-derived, and Scotch whisky, matured in oak for several years, also contains many such structures. These include gallic, ellagic, and vanillic acids, sinapaldehyde, syringaldehyde, and vanillin, among many others.^{26–28} While their concentrations in neat whisky are far lower than would be added as a matrix for MALDI, they are not very volatile and will remain in a dried sample as used for LDI. We therefore propose that matrix-free LDI will also be successful for the ionization of mature spirit drinks, such as Scotch whisky.

Comparisons of different ionization techniques have been performed before.¹² For example, ESI, APPI, and LDI were investigated and compared for the analysis of bio-oils;²⁹ MALDI and ESI of NOM were compared in another study.²² More recently we compared ESI and LDI in the analysis of NOM.²³ In all cases it was found that ESI ionized only a subset of the total chemical complexity of the samples and, therefore, that multiple ionization techniques were required for a more complete characterization of complex mixtures.

To the best of our knowledge, however, APPI, APCI, and LDI have not been applied to the analysis of food or drinks as complex mixtures using high resolution mass spectrometry in the same way as ESI. Here we report the first application of APPI, APCI, and LDI for the analysis of Scotch whisky and compare their performance to negative ionization ESI coupled to FTICR-MS. The results presented here will be applicable to most mature spirit drinks and, more generally, to all complex food and drink products.

■ EXPERIMENTAL SECTION

Samples. Scotch whisky samples ($n = 4$) were provided by the Scotch Whisky Research Institute. These were a sherry cask matured single malt (S14–1941), blended Scotch whisky (S14–1944), peated single malt (S14–1962), and a bourbon cask matured single malt (S14–2196). Samples were acidic, pH 3–5, measured with a digital pH probe. Methanol and water, both LC-MS grade, were purchased from Fisher Chemical. Nitrogen gas (99.998%) for APCI was purchased from BOC.

Mass Spectrometry. All spectra were acquired on a Bruker Solarix FTICR MS instrument equipped with an infinity cell and actively shielded 12T superconducting magnet. All spectra were acquired between 98.3 m/z and 2000.0 m/z into a 4 MWord time domain in a 1.1185 s free induction decay. All spectra had a Q1 mass of 100 m/z and were the result of 200 coadded mass analyses. The resulting resolving power was

about 300000 at 400 m/z . The four ionization sources were utilized in negative mode and without addition of chemical modifiers. Each ionization method was optimized individually.

ESI spectra were acquired in a similar fashion as described previously.¹ Briefly, the capillary voltage was set at 4000.0 V and the end plate offset at 500.0 V. The nebulizer pressure was 1.8 bar, with dry gas flow of 6.0 L/min at 180.0 °C. Samples were infused at a flow rate of 200 $\mu\text{L}/\text{h}$ and ions were accumulated for 150 ms. Samples were prepared 1:10 dilution into 50:50 methanol/water.

APPI spectra were acquired with a source equipped with a krypton lamp at 10.6 eV. The capillary voltage was set at 1500.0 V and end plate offset at 500.0 V. The nebulizer pressure was 2.5 bar at 400.0 °C, with dry gas flow of 4.0 L/min at 220.0 °C. Samples were infused at a flow rate of 2 mL/h and ions were accumulated for 600 ms. Samples were infused neat, with no addition of solvents.

APCI spectra were acquired with a corona needle discharge of 4 μA . The capillary voltage set at 4500.0 V and end plate offset at 500.0 V. The nebulizer pressure was 2.0 bar at 370.0 °C, with dry gas flow of 3.5 L/min at 220.0 °C. Samples were infused at a flow rate of 400 $\mu\text{L}/\text{h}$ and ions were accumulated for 300 ms. APCI nebulizer gas was supplied from a nitrogen gas cylinder. Samples were prepared 1:1 dilution into 50:50 methanol/water.

LDI spectra were acquired with a MALDI source fitted with a solid-state 1 kHz SmartBeam TMII laser. Laser focus was set to minimum, with 1000 shots in 1 s per scan. Laser power was set to minimum required to observe signal, however this was still high (up to 100%). Spectra were acquired with a selective accumulation of scans based upon a minimum and maximum total ion current (TIC) threshold. Samples were spotted (1 μL) directly onto a MALDI plate and allowed to air-dry. This was repeated one or more times.

Data Analysis. All spectra were acquired using *ftmsControl* 2.1 (Bruker Daltonics) and processed according to the default parameters including zero-filling once and full sine apodization prior to Fourier transformation. Spectra were further processed in *DataAnalysis* 4.2 (Bruker Daltonics) with internal quadratic recalibration based on known species and homologous series. Internal calibration lists are provided in [Table S2](#). Peak picking was performed with a signal-to-noise threshold of 4 and absolute signal magnitude greater than 2×10^6 arbitrary units, an approach recommended by Riedel and Dittmar,³⁰ well above the level of the noise across the mass range of interest.

Peaks were assigned molecular formulas based on mass accuracy with a threshold of ± 250 ppb using *Formularity*^{31,32} and the settings specified in the [Supporting Information \(SI\)](#). Formula searches were limited to CHO compounds only, however relationship searches in *Formularity* allow for some CH only assignments, in deprotonated and radical anion form. Assignments were validated using in-house Python scripts,³³ based on published guidelines,³⁴ providing similar results. Further data analysis and visualization were performed using in-house developed Python scripts.³³ Scripts and data used for this publication are available online at <https://github.com/wkew/FTMSIonisationSources>.

■ RESULTS

Spectral Acquisition. Initially, both positive and negative ionization modes were investigated. Data in positive mode with the same resolving powers were acquired for the sample set across all four ionization sources. However, the acquired

Table 1. Assigned Species and Assignment Rates of Scotch Whisky Using Four Ionization Methods^a

mode	mean # total peaks	mean% total assigned	mean # of monoisotopic hits	mean% monoisotopic radical	mean% monoisotopic deprotonated	mean error of assignment (ppb)
APCI	2795	89.9	2070	30.9	69.1	57
APPI	895	95.3	777	10.2	89.8	40
ESI	1254	82.9	875	0.8	99.2	37
LDI	4111	75.4	2664	19.8	80.2	82
overall	2264	85.9	1596	15.4	84.6	54

^aFull details for each spectrum are provided in SI, Table S3. Average numbers for the four Scotch whisky samples analyzed including isotopologues are given.

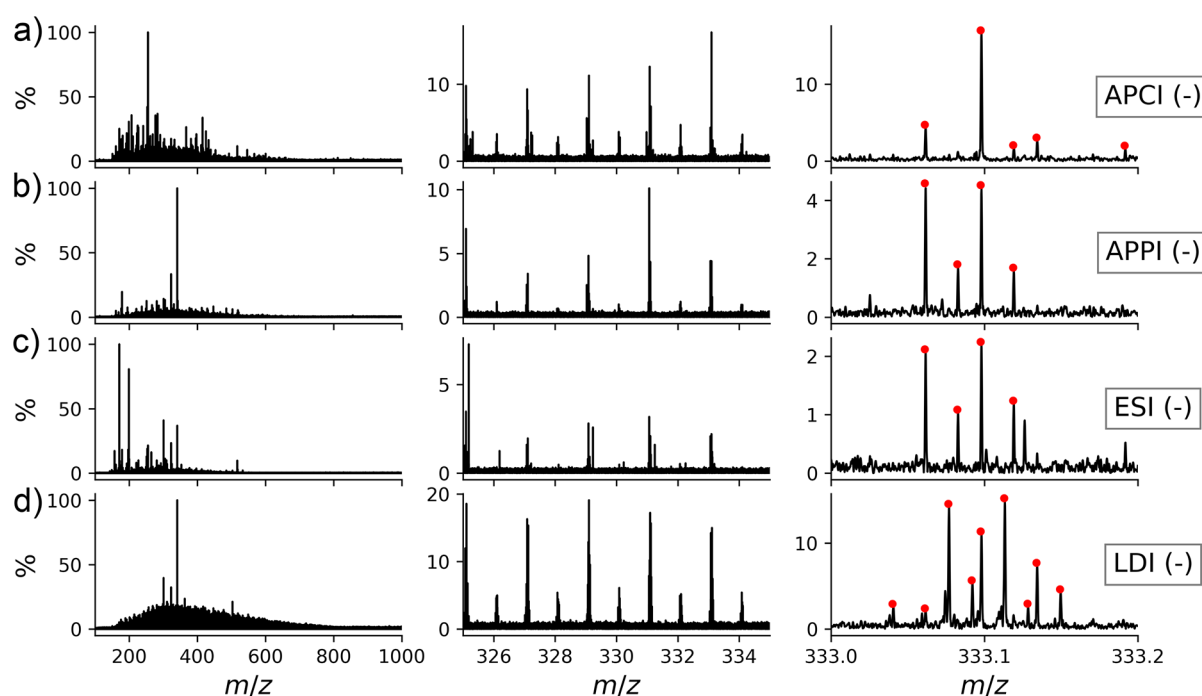


Figure 1. Mass spectra for Scotch whisky (S14–1944) acquired with APCI, APPI, ESI, and LDI (top to bottom). Columns show expansions at (a) 100–1000 m/z (left), (b) 325–335 m/z (middle), and (c) 333–333.2 m/z (right). Intensities are normalized to the largest peak in each spectrum (100%). Red dot symbols in column c (right) indicate assigned monoisotopic peaks.

positive mode data contained not just $[M + H]^+$ ions but also adducts of the form $[M + Na]^+$ and $[M + K]^+$. Negative mode spectra were exclusively assigned as $[M - H]^-$ or $[M + e]^{*-}$. In positive ion mode, the multiple ionization mechanisms resulted in increased spectral complexity, which made unambiguous formula assignment impossible at this resolving power. For a fuller discussion of this issue, see the SI. Based on these observations, only the negative mode data are analyzed and presented here.

ESI spectra of Scotch whiskeys were acquired as previously reported using our laboratory's standard protocols.¹ Samples for ESI require minimal sample volumes (10–20 μL), a factor that may be important for limited samples, such as historical or rare materials.²⁷

In contrast, APPI required significantly greater infusion rates and concentrations than ESI; a typical analysis required 150–250 μL of sample. APPI also needs a component of the sample to be ionizable below 10.6 eV, which is the power of the source lamp. To achieve this, toluene (ionization energy 8.8 eV)³⁵ is typically added as a modifier. However, water and ethanol (most of a spirit sample by volume) have ionization potentials much higher than toluene (12.7 and 10.47 eV, respectively).^{36,37} Nevertheless, APPI was successfully applied to

ionize samples of mature Scotch whisky in our laboratory with no prior sample dilution, without addition of toluene, and with higher flow rates ($\sim 33 \mu\text{L}/\text{min}$). However, it should be noted that below a sample specific flow rate threshold, no signal was obtained. In this limited sample set, it was observed that the darkest appearing samples performed best, while the lighter colored samples required the highest flow rates or even manual injection into the source. Despite ethanol's ionization energy being approximately equal to the power of the APPI lamp, we hypothesize that there is a critical concentration of a compound or compounds in Scotch whisky that can ionize and charge transfer to ionize other species. This trend of darkest samples ionizing more readily mirrored our finding with LDI (see below). Experiments with new make spirit samples failed to produce ions for APPI and LDI, limiting these ionization sources to mature spirits.

The required APCI flow rates were greater than those used for ESI (6 $\mu\text{L}/\text{min}$), but lower than needed for APPI. Likewise, more concentrated samples were required for APCI than ESI; 50–150 μL samples were typically used for APCI. Importantly, APCI requires higher purity nebulizer gas as the ionization technique can ionize residual hydrocarbon impurities present in the in-house generated nitrogen. A negative control (i.e.,

pure solvent) with in-house generated nitrogen gas confirmed the need to use a dedicated high purity nitrogen cylinder to acquire APCI spectra. Similar tests revealed no such requirement for any of the other ionization sources.

Negative mode LDI spectra were obtained readily after some method optimization: 1 μL samples (neat) were spotted onto the MALDI plate and allowed to air-dry for a few minutes. Depending on the sample, it was often necessary to reapply the sample, repeating the spotting process several times. It was found that samples lighter in color required more repeat spots to build up sufficient concentration. Due to unstable scan-to-scan ion count, a common phenomenon with LDI-based methods, the use of a TIC threshold filter prior to summing scans was required. Without this filter, the signal-to-noise suffered and peak positions varied, causing peak splitting and broadening. The use of this filter typically added a 2-fold time penalty to acquisition, further increasing when more scans were dropped. To acquire a signal, a high laser power (up to 100%) and narrow beam focus were required. No ions were observed below such laser settings. There is a risk of fragmentation associated with the higher laser powers utilized. However, as with our previous study,²³ no indications of ion fragmentation were observed in these experiments.

Assessing the Quality of the Mass Spectra. All acquired spectra were of high quality, with a resolving power of about 300000 at 400 m/z and a median signal-to-noise ratio at 401 m/z of between 16 (LDI) and 35 (APPI). As acquisition settings were similar and digitizer settings identical, all spectra have comparable resolution and noise levels. Across the four whisky samples, there were on average between 895 (APPI) and 4111 (LDI) peaks picked. Of these, between 75% (LDI) and 95% (APPI) were assigned formulas within the error thresholds (Tables 1 and S3).

Examples for one whisky sample at three levels of expansion (100–1000, 325–335, and 333.0–333.2 m/z) are shown in Figure 1a–c, respectively. For all ionization modes, the spectra are dominated by a small number of abundant peaks, with most of the complexity at much lower relative abundance. For example, for APCI, the most abundant peak corresponds to 255.23295 m/z ($[\text{C}_{16}\text{H}_{31}\text{O}_2]^-$, 10 ppb), likely a fatty acid such as palmitic acid. As can be seen in the Figure 1b, there are a multitude of peaks at each odd m/z , with much smaller peaks at each even m/z corresponding to CHO species and their ^{13}C -containing isotopologues, respectively. This trend is repeated for all ionization modes, nevertheless, the peak abundance at even m/z varies, for example, more abundant peaks were seen in the APCI and LDI spectra than in the spectra acquired by the other two methods. Many of the signals at even m/z were assigned as radical anions, especially in APCI and LDI. Furthermore, the lack of peaks between each nominal mass confirms that all species are singly charged. These observations agree with previous finding for negative mode ESI spectra of both Scotch whisky and other complex mixtures.^{1,23} Nitrogen-containing species were neither detected nor assigned.

The spectrum acquired using APPI is dominated by a species at 341.10893 m/z ($[\text{C}_{12}\text{H}_{21}\text{O}_{11}]^-$, 26 ppb), which corresponds to a molecular formula of a disaccharide. This compound also dominates the LDI spectrum. Neither APPI nor LDI contain fatty acid-type signals of any significant abundance, suggesting that these ionization sources may ionize different classes of compounds, such as polyphenols and lignin derivatives.

The spectrum obtained using ESI was consistent with previously published data.¹ It features two large signals at 171.13905 m/z and 199.17035 m/z ($[\text{C}_{10}\text{H}_{19}\text{O}_2]^-$, 13 ppb and $[\text{C}_{12}\text{H}_{24}\text{O}_2]^-$, 12 ppb), corresponding to two fatty acids. The next most abundant signals are at 300.99900 m/z and 341.10893 m/z ($[\text{C}_{14}\text{H}_5\text{O}_8]^-$, 32 ppb and $[\text{C}_{12}\text{H}_{21}\text{O}_{11}]^-$, 26 ppb), corresponding to ellagic acid (a known cask extractive), and a disaccharide (as observed in the APPI data).

The LDI spectrum was the most distinct among the four ionization sources. Aside from the previously mentioned disaccharide (341.10893 m/z) and ellagic acid (300.99900 m/z), the spectrum has a skewed normal distribution of signal intensities. This type of mass spectrum profile is more typically observed for NOM. Given the compounds present in Scotch whisky are known to exist at a wide range of concentrations, this relatively homogeneous distribution of abundances suggests an even less quantitative ionization mechanism for LDI than ESI. Of all the ionization techniques used, the LDI spectrum had the highest signal abundance (see Figure 1) and the most peaks at this single nominal mass. This was due to LDI presenting a more normally distributed spectrum; the other ionization sources were not normally distributed.

The final expansions of the spectra within 0.3 m/z at 333 m/z are shown in Figure 1c; Table 2 contains molecular formulas

Table 2. Formula Assignments for Scotch Whisky (S14-1944) and Mass Errors for APCI, APPI, ESI, and LDI between 333.0 and 333.3 m/z ^a

m/z	formula ^b	error (ppm)	APCI	APPI	ESI	LDI
333.04049	$\text{C}_{19}\text{H}_{10}\text{O}_6$	-0.09				X
333.06160	$\text{C}_{16}\text{H}_{14}\text{O}_8$	-0.02	X	X	X	X
333.07685	$\text{C}_{20}\text{H}_{14}\text{O}_3$	-0.02				X
333.08273	$\text{C}_{13}\text{H}_{18}\text{O}_{10}$	-0.01		X	X	
333.09215	$\text{C}_{24}\text{H}_{14}\text{O}_2$	-0.13				X
333.09798	$\text{C}_{17}\text{H}_{18}\text{O}_7$	-0.02	X	X	X	X
333.11327	$\text{C}_{21}\text{H}_{18}\text{O}_4$	-0.11				X
333.11911	$\text{C}_{14}\text{H}_{22}\text{O}_9$	-0.02	X	X	X	
333.12848	$\text{C}_{25}\text{H}_{18}\text{O}$	0.04				X
333.13436	$\text{C}_{18}\text{H}_{22}\text{O}_6$	0.00	X			X
333.14966	$\text{C}_{22}\text{H}_{22}\text{O}_3$	-0.13				X
333.19187	$\text{C}_{16}\text{H}_{30}\text{O}_7$	0.01	X			

^aCrosses in the final four columns indicate a peak that was assigned in the given spectrum. ^bShown in neutral molecular form.

identified by all ionization techniques in this region. In the APCI spectrum all five peaks have been assigned monoisotopic molecular formulas. The APPI expansion has a similar appearance to the APCI spectrum with three out of four assigned peaks common with the APCI data. The ESI spectrum displays six peaks, however, only four were assigned: these were the same species as assigned in the APPI spectrum. LDI showed the largest number: nine peaks were observed and assigned. Only two of these were common with the other three spectra, and a third was common with a formula identified in the APCI spectrum.

Formula Assignment. All 16 spectra were assigned simultaneously, with peak alignment prior to formula assignment. Formulas were assigned from deprotonated ions and radical anions, as described in more detail in the Experimental Section and the SI. Table 1 shows the number of assigned molecular formulas for each ionization source. These numbers represent the mean across the four Scotch whisky samples

analyzed. Also shown is the average percentage of mono-isotopic peaks assigned as radical anions, average percentage of assigned peaks, including isotopologues, per ionization source, and the average assignment error in parts-per-billion (ppb). The individual results for each spectrum are detailed in Table S3.

All ionization sources assigned more than 75% molecular formula across the average of four whisky samples, which represent excellent assignment rates for MS analysis of complex mixtures. All assignments were made with a maximum error threshold of ± 250 ppb, and the average for all ionization modes was considerably lower than that threshold. The average distributions of errors achieved using each ionization technique are shown in Figure S1. LDI has the broadest error distribution, with APPI and ESI having the narrowest error distributions overall. However, the distributions of errors appear largely normally distributed around 0 ppm for all ionization modes, indicative of correctly calibrated data. Overall, an average of 86% of peaks were assigned formula with a mean error of 54 ppb. These statistics give high confidence in the assignment of data.

Across all 16 spectra acquired, including four samples and four ionization modes, there were a total of 20809 monoisotopic molecular formulas assigned. Accounting for the duplication of radical and deprotonated ions, 3993 were unique molecular formulas. LDI and APCI had the greatest number of peaks and assignments; however, APPI and ESI had better rates of assignment than LDI. APPI had a very high assignment rate (95%), with an average error of only 40 ppb.

The assignment of radical anions was necessary to comprehensibly interpret the acquired data and to achieve high formula assignment rates, especially for APCI and LDI. As shown in Table 1, radical anions were assigned in each ionization mode. Radical anions and the first isotopic peak of the same compounds were well resolved; an example is shown in Figure S2. APCI had an average of 31% of monoisotopic peaks assigned as radicals, with 20% for LDI and 10% for APPI. Less than 1% of monoisotopic peaks were assigned as radicals for ESI. However, these radical anions do not constitute a different chemistry to those assigned as deprotonated ions. Table S4 shows the numbers of formulas that were uniquely identified from radical anion assignments. This was most significant for APCI, where 6% of the unique molecular formulas were only identified as radical anions, but even this is a relatively small number. Most compounds found as radical anions were, therefore, also found as deprotonated ions. Across all assigned formulas, radical ions had a median ion abundance of 64% of that of their equivalent deprotonated ions. All subsequent analyses are based on nonduplicated formula lists, and reported ion abundances are the mean of the radical and deprotonated forms when both forms were assigned.

To investigate the intersections of formulas assigned between each ionization mode, *UpSet* plots were utilized.³⁸ It is generally not possible to accurately plot scaled three set Venn diagrams using circles and impossible to even approximate this for four sets.^{38,39} Instead, the *UpSet* plots are an attractive alternative to represent the size of intersections across many sets, as they display the exclusive intersections of sets of data. The *UpSet* plot shown in Figure 2 presents a cumulative account of individual ionization methods across all four samples. LDI has the most unique formulas assigned, whereas APPI provides the least (1424 compared to

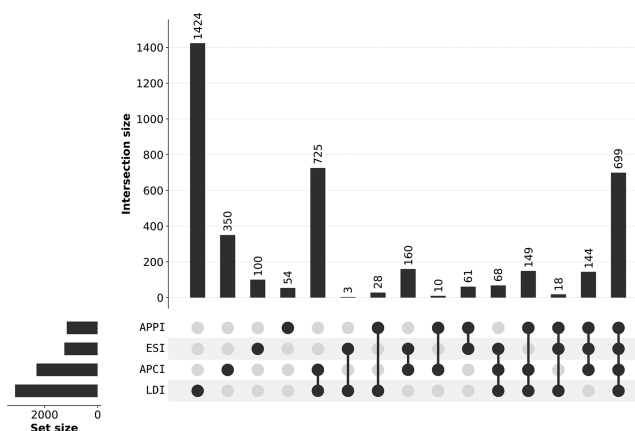


Figure 2. *UpSet* plots showing intersections of each ionization source. Set size on the left indicates the number of unique formulas for each source across the four whisky samples. Vertical bar plots indicate the number of formulas found in each exclusive intersection.

54 formulas). APCI and LDI had the greatest number of common formulas in their pairwise intersection (725), and overall, there were 699 formulas common to all negative mode ionization sources. Pairwise, ESI and LDI are least similar, which is to be expected due to their fundamentally different ionization mechanisms. Similar results were previously obtained for SRFA.²³ The presented *UpSet* plot clearly highlights the complementary information provided by the four ionization sources in negative mode.

Additional comparisons can be made on the level of individual samples. The distribution of the number of times formulas were assigned across the 16 spectra is shown in Figure S3. There were 663 unique formulas assigned in only one spectrum, meaning that over 83% of formulas were identified in at least two spectra. Only 178 of the unique formulas were identified in all 16 spectra. The distribution of unique formulas across spectra for each sample is shown in Figure S4. These results highlight that there is significant chemical diversity between the whisky samples and between the ionization sources.

Chemical Diversity. While formula intersections give some information about chemical diversity of the selected four Scotch whisky samples, as revealed by the different ionization modes, complex mixtures are rarely analyzed on an individual formula level. Instead, it is more typical to investigate the distribution of heteroatomic classes or to visualize the data through van Krevelen diagrams and double bond equivalence (DBE) versus carbon number plots.

The heteroatomic, or oxygen, class distributions for the four ionization modes extend to O19, as shown in Figure 3. Formulas were assigned above this class, up to O25; however, only 34 formulas out of 20809 were assigned above O19, and the figure was truncated accordingly. Similarly, seven CH-only formulas were assigned; however, these were also excluded from this figure.

LDI clearly contains the most formulas, and their class distribution extends from O1 upward. LDI, along with APPI, presents a normal distribution of oxygen classes centered around O10 and O11, respectively. APPI has very few formulas identified below O4. It appears to be preferably ionizing oxygen-rich aromatic compounds, for example, lignin-derived compounds. APCI, like LDI, has formulas extending from O1. APCI presents a bimodal distribution around O4 and O12.

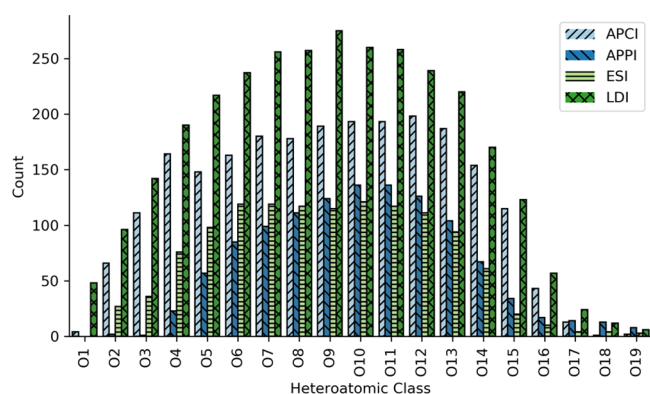


Figure 3. Heteroatomic class histogram for ionization modes. Y-Axis is the count of formulas containing the given number of oxygens. Each unique formula within each ionization mode across all samples is counted only once; for example, if the same formula appears in more than one sample in a given ionization source, it only counts once.

Finally, ESI presents an almost bimodal distribution around O6 and O10, consistent with our previous results.¹ Counts for oxygen classes above O15 drop off significantly for all ionization modes. This is in part due to instrumental settings, particularly the optimized mass range during analysis. It is interesting that the distribution of oxygen classes is similar across different ionization modes (ESI, LDI, and APPI) and that APCI is the most unusual, with a local maximum at O4. LDI also shows a higher abundance of compounds below the O4 class, as seen previously in the LDI spectra of SRFA.²³

The van Krevelen diagrams provide a simple representation of the CHO chemical space, as reported by the mass spectra.⁴⁰ This is shown for all ionization sources in Figure 4 as a

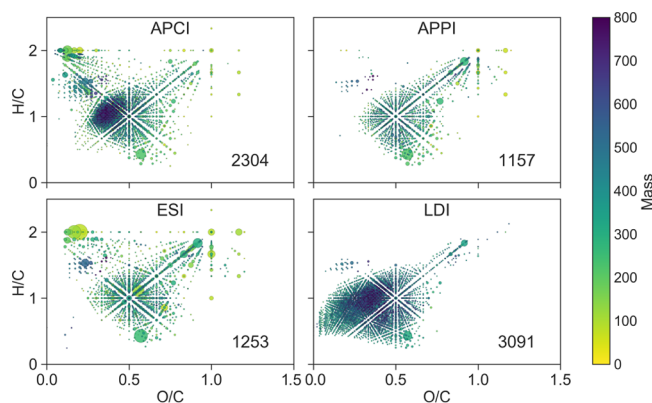


Figure 4. Van Krevelen diagrams for each ionization source. Each assignment from individual ionization modes was plotted with the size of the glyph representing the median abundance across the four whisky samples. The color represents the mass of the peak. The number in the bottom right corner shows the number of unique formulas identified for each ionization source across four samples.

cumulative plot for all four whiskies, allowing their convenient visual comparison. The styling of the figure is as previously reported.^{1,33} Additionally, interactive van Krevelen plots are available online at <https://github.com/wkew/FTMSIonisationSources>.³³ The van Krevelen representation of the ESI data is similar to our previous interpretation of ESI data set of 85 Scotch whisky samples,¹ with several lower mass species at high H/C ratio and low O/C ratio corresponding to fatty acids or alcohols. The top right, high H/C and high O/C

correspond to carbohydrates, and the diagonal toward the center likely indicates carbohydrate breakdown products. The central star region, at H/C 1 and O/C 0.5, is occupied by cask extractives, likely lignin-derived compounds. For a more detailed interpretation of ESI-based van Krevelen diagrams of 85 Scotch whisky samples, refer to Kew et al.¹

ESI shares some similarities with APCI and APPI, with the APCI containing more of the low O/C species, while APPI is dominated by the central star-to-carbohydrate region. The central star region is likely to contain UV active compounds, which are preferentially ionized using APPI. As color is an area of interest to the mature spirits industry, this is potentially a useful finding. APCI has nearly twice as many assignments than ESI and APPI; however, it does not appear to be covering a significantly larger chemical space. There are more species identified around H/C 1.4 and O/C 0.2 for the APCI, exemplified by the molecular formula $C_{30}H_{46}O_7$ and related compounds. These compounds are likely to be triterpenoids, as previously suggested.^{1,41,42} Their increased number in the APCI spectra will be useful for the investigation of the wood extracts chemistry. LDI shows the greatest difference from ESI; it contains nearly three times as many formulas, has no fatty acid region, and has only a nominal amount of carbohydrate and trend line assignments. It is heavily dominated by species with O/C ratios below 0.5 and H/C ratios below 1.2. A similar trend was observed in our comparisons of ESI and LDI spectra of SRFA.²³

The DBE versus carbon number plots are shown in Figure 5. Again, the ESI results show a similar profile as reported

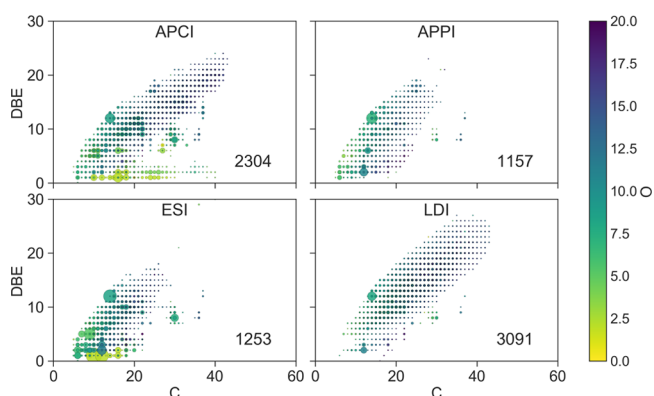


Figure 5. DBE vs C number plots for each ionization source. Each assignment from individual ionization modes was plotted with the size of the glyph representing the median abundance across the four whisky samples. As DBE does not account for oxygen, the color represents the oxygen count of the peak. The number in the bottom right corner shows the number of unique formulas identified for each ionization source across four samples.

previously.¹ ESI plots share a similar profile to APPI, however, the APPI data do not contain many of the low DBE and low oxygen species, that is, the fatty acid compounds. Both APPI and ESI do not extend much beyond C30 and DBE of 18. There is some similarity between the APCI and ESI data, however, APCI shows a large DBE and C number range, extending up to C40 and a DBE of 25. It includes higher carbon number compounds with low DBE and low oxygen numbers, which may be longer chain unsaturated fatty acid-type species, as well as higher DBE species with higher oxygen numbers, which may be complex aromatic compounds. LDI,

again, is the most different. Like APPI, it lacks the fatty acid species, however, it extends beyond C40 and up to DBE 28 in a largely normal distribution. Again, the DBE analysis shows that there is an overlap between the ionization techniques, but complementary data are to be obtained by each technique.

Additional visualization of the results obtained by different ionization modes is presented in the SI. A van Krevelen diagram for the 699 formulas common to all ionization modes is shown in Figure S5. These are likely to be wood extractive compounds, lignin derivatives, and glycosides. Van Krevelen and DBE versus C number plots showing the unique formula for each ionization mode are shown in Figures S6 and S7, respectively. These diagrams reaffirm the analysis presented above and show, for example, that LDI and APCI produced most of the unique formulas, typically with a low O/C ratio (both techniques) and a H/C ratio below 1 (LDI) or between 1 and 2 (APCI). They also illustrate nicely the formula intersections.

Another metric that can be used to classify the compounds based on their molecular formulas is the aromaticity index (AI). AI categorizes the compounds as nonaromatic, aromatic, and condensed aromatics. It was calculated (as the modified AI)⁴³ for all assigned formulas. The relative percentages of formulas corresponding to these compound classes are shown in Figure S8. The relative AI distributions among the four ionization sources confirmed the van Krevelen analysis; ESI is most similar to APCI and APPI in terms of relative numbers of aromatic and nonaromatic species identified. LDI is different, with nearly 50% of assigned formulas described as aromatic or condensed aromatic. This prevalence of aromatic or condensed aromatic compounds observed by LDI was even more pronounced (~92%) in the LDI spectra of SFRA.²³ A comparison of the corresponding van Krevelen diagrams showed that, unlike in the SRFA sample, compounds with $H/C \geq 1$ were present in significant numbers in the whisky samples. These compounds reflect the higher content of nonaromatic moieties in whisky samples, which are ionizable by LDI.

CONCLUSIONS

Only high-resolution mass spectrometry can resolve the thousands of compounds present in complex mixtures, such as Scotch whisky. However, the de facto standard electrospray ionization is only one of several methods that can be used for this analysis. In this work we have found that APCI, APPI, and LDI in the negative mode are all viable alternatives to negative mode ESI, providing significant complementary information. Assignment of thousands of deprotonated and radical anions with a parts-per-billion mass accuracy was possible, allowing for a comparison of the ionization techniques at the chemical level. All four ionization sources produced spectra of Scotch whisky that were dominated by CHO compounds; however, there is great diversity, as shown by visualizing the intersections of these spectra and characterizing their chemical nature. ESI and APCI often contain significant fatty acid signals, and while APPI has the fewest peaks, it may be the most appropriate technique for investigations of color active compounds. The techniques and results presented here are broadly applicable to other mature spirit drinks and, in a more general context, will aid the analysis of other complex mixtures.

ASSOCIATED CONTENT

Supporting Information

The Supporting Information is available free of charge on the ACS Publications website at DOI: 10.1021/acs.analchem.8b01446.

Additional discussion on positive mode data acquisition; calibration lists; formula assignment parameters; assignment mass error distributions; radical anion assignments; further formula assignment statistics; visualization of common unique and common formulas assigned; and aromaticity index distributions (PDF).

AUTHOR INFORMATION

Corresponding Authors

*Tel.: +44(0)131 650 4742. E-mail: dusan.uhrin@ed.ac.uk.

*Tel.: +44(0)131 650 4808. E-mail: dave.clarke@ed.ac.uk.

ORCID

Dušan Uhrin: 0000-0002-0254-4971

Notes

The authors declare no competing financial interest.

ACKNOWLEDGMENTS

Thanks to Dr. Faye Cruickshank, Dr. John Blackburn, and Alan Smith for helpful discussions in data collection and analysis. Thanks also to the Scotch Whisky Research Institute for providing the samples used in this study. Research funded by Biotechnology and Biological Sciences Research Council, Grant No. BB/L016311/1.

REFERENCES

- (1) Kew, W.; Goodall, I.; Clarke, D.; Uhrin, D. *J. Am. Soc. Mass Spectrom.* **2017**, *28*, 200–213.
- (2) Garcia, J. S.; Vaz, B. G.; Corilo, Y. E.; Ramires, C. F.; Saraiva, S. A.; Sanvido, G. B.; Schmidt, E. M.; Maia, D. R. J.; Cosso, R. G.; Zacca, J. J.; et al. *Food Res. Int.* **2013**, *51*, 98–106.
- (3) Roullier-Gall, C.; Signoret, J.; Hemmler, D.; Witting, M. A.; Kanawati, B.; Schäfer, B.; Gougeon, R. D.; Schmitt-Kopplin, P. *Front. Chem.* **2018**, *6*, 1–11.
- (4) Møller, J. K. S.; Catharino, R. R.; Eberlin, M. N. *Analyst* **2005**, *130*, 890.
- (5) Araújo, A. S.; da Rocha, L. L.; Tomazela, D. M.; Sawaya, A. C. H. F.; Almeida, R. R.; Catharino, R. R.; Eberlin, M. N. *Analyst* **2005**, *130*, 884–889.
- (6) Cooper, H. J.; Marshall, A. G. *J. Agric. Food Chem.* **2001**, *49*, 5710–5718.
- (7) Jeandet, P.; Heinzmann, S. S.; Roullier-Gall, C.; Cilindre, C.; Aron, A.; Deville, M. A.; Moritz, F.; Karbowiak, T.; Demarville, D.; Brun, C.; et al. *Proc. Natl. Acad. Sci. U. S. A.* **2015**, *112*, 5893–5898.
- (8) Roullier-Gall, C.; Witting, M.; Moritz, F.; Gil, R. B.; Goffette, D.; Valade, M.; Schmitt-Kopplin, P.; Gougeon, R. D. *Food Chem.* **2016**, *203*, 207–215.
- (9) Marshall, J. W.; Schmitt-Kopplin, P.; Schuetz, N.; Moritz, F.; Roullier-Gall, C.; Uhl, J.; Colyer, A.; Jones, L. L.; Rychlik, M.; Taylor, A. *J. Food Chem.* **2018**, *242*, 316–322.
- (10) Ibáñez, C.; Simó, C.; García-Cañas, V.; Acunha, T.; Cifuentes, A. *Anal. Bioanal. Chem.* **2015**, *407*, 6275–6287.
- (11) Rychlik, M.; Kanawati, B.; Schmitt-Kopplin, P. *TrAC, Trends Anal. Chem.* **2017**, *96*, 22–30.
- (12) Hertkorn, N.; Frommberger, M.; Witt, M.; Koch, B. P.; Schmitt-Kopplin, P.; Perdue, E. M. *Anal. Chem.* **2008**, *80*, 8908–8919.
- (13) Dier, T. K. F.; Egele, K.; Fossog, V.; Hempelmann, R.; Volmer, D. A. *Anal. Chem.* **2016**, *88*, 1328–1335.

- (14) McClelland, D. J.; Motagamwala, A. H.; Li, Y.; Rover, M. R.; Wittrig, A. M.; Wu, C.; Buchanan, J. S.; Brown, R. C.; Ralph, J.; Dumesic, J. A.; et al. *Green Chem.* **2017**, *19*, 1378–1389.
- (15) Chiaberge, S.; Fiorani, T.; Savoini, A.; Bionda, A.; Ramello, S.; Pastori, M.; Cesti, P. *Fuel Process. Technol.* **2013**, *106*, 181–185.
- (16) Kim, Y. H.; Kim, S. *J. Am. Soc. Mass Spectrom.* **2010**, *21*, 386–392.
- (17) McKenna, A. M.; Williams, J. T.; Putman, J. C.; Aeppli, C.; Reddy, C. M.; Valentine, D. L.; Lemkau, K. L.; Kellermann, M. Y.; Savory, J. J.; Kaiser, N. K.; et al. *Energy Fuels* **2014**, *28*, 2454–2464.
- (18) Krajewski, L. C.; Rodgers, R. P.; Marshall, A. G. *Anal. Chem.* **2017**, *89*, 11318–11324.
- (19) Smith, D. F.; Podgorski, D. C.; Rodgers, R. P.; Blakney, G. T.; Hendrickson, C. L. *Anal. Chem.* **2018**, *90*, 2041–2047.
- (20) Hurtado-Fernández, E.; Pacchiarotta, T.; Mayboroda, O. A.; Fernández-Gutiérrez, A.; Carrasco-Pancorbo, A. *Food Res. Int.* **2014**, *62*, 801–811.
- (21) Hurtado-Fernández, E.; Pacchiarotta, T.; Mayboroda, O. A.; Fernández-Gutiérrez, A.; Carrasco-Pancorbo, A. *Anal. Bioanal. Chem.* **2015**, *407*, 547–555.
- (22) Cao, D.; Huang, H.; Hu, M.; Cui, L.; Geng, F.; Rao, Z.; Niu, H.; Cai, Y.; Kang, Y. *Anal. Chim. Acta* **2015**, *866*, 48–58.
- (23) Blackburn, J. W. T.; Kew, W.; Graham, M. C.; Uhrin, D. *Anal. Chem.* **2017**, *89*, 4382–4386.
- (24) Witt, M.; Fuchser, J.; Koch, B. P. *Anal. Chem.* **2009**, *81*, 2688–2694.
- (25) Bell, N. G. A.; Michalchuk, A. A. L.; Blackburn, J. W. T.; Graham, M. C.; Uhrin, D. *Angew. Chem., Int. Ed.* **2015**, *54*, 8382–8385.
- (26) Aylott, R.; Mackenzie, W. J. *Inst. Brew.* **2010**, *116*, 215–229.
- (27) Pryde, J.; Conner, J.; Jack, F.; Lancaster, M.; Meek, L.; Owen, C.; Paterson, R.; Steele, G.; Strang, F.; Woods, J. J. *Inst. Brew.* **2011**, *117*, 156–165.
- (28) Kew, W.; Bell, N. G. A.; Goodall, I.; Uhrin, D. *Magn. Reson. Chem.* **2017**, *55*, 785–796.
- (29) Hertzog, J.; Carré, V.; Le Brech, Y.; Mackay, C. L.; Dufour, A.; Mašek, O.; Aubriet, F. *Anal. Chim. Acta* **2017**, *969*, 26–34.
- (30) Riedel, T.; Dittmar, T. *Anal. Chem.* **2014**, *86*, 8376–8382.
- (31) Tolić, N.; Liu, Y.; Liyu, A.; Shen, Y.; Tfaily, M. M.; Kujawinski, E. B.; Longnecker, K.; Kuo, L.-J.; Robinson, E. W.; Paša-Tolić, L.; et al. *Anal. Chem.* **2017**, *89*, 12659–12665.
- (32) Kujawinski, E. B.; Behn, M. D. *Anal. Chem.* **2006**, *78*, 4363–4373.
- (33) Kew, W.; Blackburn, J. W. T.; Clarke, D. J.; Uhrin, D. *Rapid Commun. Mass Spectrom.* **2017**, *31*, 658–662.
- (34) Kind, T.; Fiehn, O. *BMC Bioinf.* **2007**, *8*, 105.
- (35) Lu, K. T.; Eiden, G. C.; Weisshaar, J. C. *J. Phys. Chem.* **1992**, *96*, 9742–9748.
- (36) Rabalais, J. W.; Debies, T. P.; Berkosky, J. L.; Huang, J. J.; Ellison, F. O. *J. Chem. Phys.* **1974**, *61*, 516–528.
- (37) Refaey, K. M. a.; Chupka, W. A. *J. Chem. Phys.* **1968**, *48*, 5205–5219.
- (38) Lex, A.; Gehlenborg, N.; Strobelt, H.; Vuillemot, R.; Pfister, H. *IEEE Trans. Vis. Comput. Graph.* **2014**, *20*, 1983–1992.
- (39) Chen, H.; Boutros, P. C. *BMC Bioinf.* **2011**, *12*, 35.
- (40) Kim, S.; Kramer, R. W.; Hatcher, P. G. *Anal. Chem.* **2003**, *75*, 5336–5344.
- (41) Marchal, A.; Waffo-Téguo, P.; Génin, E.; Méryllon, J. M.; Dubourdieu, D. *Anal. Chem.* **2011**, *83*, 9629–9637.
- (42) Marchal, A.; Prida, A.; Dubourdieu, D. *J. Agric. Food Chem.* **2016**, *64*, 618–626.
- (43) Koch, B. P.; Dittmar, T. *Rapid Commun. Mass Spectrom.* **2006**, *20*, 926–932.